**Ind. J. Pharm. Edu. Res., 2026; 60(3s):s1215-s1230.**
https://www.ijper.org

Original Article

# Insulin-Sensitizing Effect of *Buchanania lanzan* Leaf Extract: Integrated Computational and *in vivo* Evidence

**Rubina Usman Watangi[1], Nayeem Ashrafali Khatib[1,*], Sunil Tuakaram Galatage[2], Arehalli Sidramappa Manjappa[2], Tufailahmad Basheerahmad Sajjan[1], Ekta Uday Kotharkar[1], Rajkumar Sanjay Patil[1]**

[1]Department of Pharmacology, KLE College of Pharmacy, Belagavi; KLE Academy of Higher Education and Research, Belagavi, Karnataka, INDIA.
[2]Department of Pharmaceutics, Vasantidevi Patil Institute of Pharmacy, Kodoli, Kolhapur, Maharashtra, INDIA.

## ABSTRACT

**Background:** *Buchanania lanzan* Spreng. is a plant having anti-diabetic, anti-inflammatory properties. **Aim:** The aim of this research is to assess methanolic extract of *Buchanania lanzan* leaves for insulin sensitivity in diet induced insulin resistance rats and to elucidate the mechanisms of *Buchanania lanzan* phytoconstituents. **Materials and Methods:** Bioactive compounds from *Buchanania lanzan* were retrieved from phytochemical databases and published literature. Docking was performed using GNU Parallel-based pipeline- Parallelized Open Babel & AutoDock suite Pipeline. Diet-induced insulin resistance model was used to evaluate the *Buchanania lanzan* for insulin sensitivity followed by an oral glucose tolerance test, fasting glucose, and fasting insulin. Biochemical parameters such as glycogen content, glucose uptake, Tumor Necrosis Factor-α (TNF-α), antioxidant biomarkers, and lipid profiles were quantified along with histology study on the liver and pancreas. **Results:** Pathways enrichment analysis of 33 targets identified 14 molecular pathways associated with insulin resistance and its complications. It was found that the PI3K-Akt signaling pathway had the lowest false discovery rate and the highest gene count. Myricetin 3-galactoside-3'-rhamnoside (-8.9 kcal/mol), kaempferol-7-o'glucoside (-8.5 kcal/mol), myricetin 3-galactoside-3'-rhamnoside (-7.6 kcal/mol) were identified as best hits against Peroxisome Proliferator-Activated Receptor Gamma (PPARG), Dipeptidyl Peptidase-4 (DPP4), and Protein Tyrosine Phosphatase Non-Receptor Type 1 (PTPN1) respectively that formed the highest interactions with active site residues compared to standard molecules. These results were correlated with the results of *in-vivo* study. *Buchanania lanzan* lowered elevated blood glucose levels by stimulating insulin secretion, played a vital role in preserving liver and islet cells, regulating glycolysis or gluconeogenesis, increasing glucose uptake in skeletal muscles, and decreasing TNF-α levels in serum. **Conclusion:** Results confirmed that *Buchanania lanzan* exhibit significant anti-insulin resistance, anti-inflammatory, anti-hyperlipidemic, anti-hyperglycemic, and antioxidant activities. These effects are likely ascribed to the presence of flavonoids in the leaves. *Buchanania lanzan* potentially modulate key proteins such as PPARG, DPP4, and PTPN1, thereby enhancing insulin sensitivity through the activation of the PI3K-Akt signaling pathway.

**Keywords:** *Buchanania lanzan* Leaves, Flavonoids, Insulin Resistance, Network Pharmacology.

**Correspondence:**
**Dr. Nayeem A. Khatib**
Department of Pharmacology, KLE College of Pharmacy, Belagavi; KLE Academy of Higher Education and Research, Belagavi, Karnataka, INDIA.
Email: khatibbgm@gmail.com

**Received:** 22-12-2025;
**Revised:** 05-02-2026;
**Accepted:** 13-04-2026.

## INTRODUCTION

Insulin Resistance (IR) is a pivotal factor in the development of various pathophysiologic conditions, including Polycystic Ovary Syndrome (PCOS), hypertension, hyperlipidemia, and atherosclerosis, as well as being a cornerstone of Type 2 Diabetes Mellitus (T2DM) pathogenesis. In T2DM, the inability of the tissues to utilize insulin effectively leads to hyperglycemia. Although the precise mechanisms linking IR to these disorders remain incompletely understood, research indicates that inflammation, oxidative stress, and alterations in lipid metabolism contribute significantly.[1] Obesity, affecting one-third of the global population, exacerbates IR and its associated health risks. By 2030, projections suggest that 20% of adults worldwide will be obese and 38% overweight, highlighting the urgent need for effective intervention.[2] Both obesity and T2DM exhibit IR, characterized by diminished insulin-driven glucose transport and metabolism in adipose tissues and skeletal muscle, along with inadequate inhibition of hepatic glucose output.[3]

Diet plays a crucial role in exacerbating IR and related metabolic disorders. High intake of fructose and saturated fats, common in processed foods, increases the risk of obesity and metabolic diseases such as insulin resistance, hyperinsulinemia, hypertriglyceridemia, and hyperglycemia.[4] Saturated fats, which

**DOI:** 10.5530/ijper.20264345

are present in animal products and specific plant-based oils, increase the levels of Low-Density Lipoprotein (LDL) heightening the risk of heart disease and stroke.[5,6] Concurrent consumption of saturated fats and sugars exacerbates health risks, particularly due to the potential accumulation of liver fat.[4] Managing IR is essential in treating T2DM and preventing associated conditions. Medications like metformin and Thiazolidinediones (TZDs) are commonly used for this purpose.[7] A multifaceted approach encompassing dietary modifications, pharmacological intervention, and lifestyle changes is necessary for effective diabetes management.[8,9]

Phytoconstituents such as polyphenols and flavonoids demonstrate promising results in managing diabetes by improving insulin sensitivity, promoting insulin secretion, inhibiting hepatic glucose production, delaying carbohydrate absorption, and reducing inflammation and oxidative stress.[10,11] Dysregulation of signaling pathways, including oxidative stress, inflammatory, and insulin signaling pathways, underlies IR at the molecular level.[12] *Buchanania lanzan* (BL), a sensitive medicinal plant, possesses various pharmacological properties, including anti-diabetic, antioxidant, wound healing, anticancer, and larvicidal activities. Its leaves contain secondary metabolites such as phenols, glycosides, flavonoids, tannins, carbohydrates, and saponins. Previous studies have reported the methanolic extract of BL exhibiting anti-diabetic, antioxidant, and anti-hyperlipidemic activities.[13-15] Utilizing a systems biology approach to understand the molecular pathways underlying the anti-IR activity of BL leaves could unveil novel therapeutic targets for diabetes and related metabolic diseases.[14,16] This comprehensive understanding is essential for the advancement of effective treatments and the development of herbal medicines in the public health sector.

## MATERIALS AND METHODS

### Data mining, network construction

Bioactive constituents from BL leaves were retrieved available phytochemical databases viz., PCIDB (https://www.genome.jp/db/pcidb), ChEBI (https://www.ebi.ac.uk/chebi/init.do), and Dr. Dukes (https://phytochem.nal.usda.gov/phytochem/search). Swiss Target Prediction (http://www.swisstargetprediction.ch/) and Binding DB (https://www.bindingdb.org/) were used to predict the probable protein targets and the prediction was limited to "Homo sapiens". IR-linked targets were screened from Gene Cards using "Insulin Resistance" as the key term and a with high-confidence association score ≥20 (Table 1). The above-selected protein targets of phytocompounds Protein-Protein Interactions (PPIs) data were analyzed by STRING (https://string-db.org/) database. The Cytoscape version 3.7.2 was used to build the network that links compounds, targets, and pathways.

### Active site identification and docking

The putative active/binding sites of the selected protein structures were predicted using the P2Rank server (https://prankweb.cz/), which employs machine learning-based pocket detection algorithms. The identified binding pockets were prioritized based on their ranking scores and druggability estimates provided by the server. Based on previous reports, we prioritized PPARG (PDB ID: 3U9Q), DPP4 (PDB ID: 6B1E), and PTPN1 (PDB ID: 3EB1) because these targets are involved in the regulation of glucose and lipid metabolism and play key roles in the development and modulation of insulin resistance.[17] Pioglitazone, Sitagliptin and 4-[3-(dibenzylamino)phenyl]-2,4-dioxobutanoic acid were used as standard molecules of PPARG, DPP4 and PTPN1 respectively. For molecular docking, a GNU Parallel-based POAP pipeline integrating Open Babel (for ligand preparation and format conversion) and the Auto Dock suite (for docking simulations) was employed, enabling high-throughput virtual screening in an optimally parallelized manner. Ligand structures were energy-minimized using the MMFF94 force field in Open Babel prior to docking. Docking was carried out using Auto Dock Vina with an exhaustiveness parameter set to 100 to ensure extensive conformational sampling.[18] For each ligand, nine docking conformations (poses) were generated. Among these, the conformation that has the lowest binding energy and RMSD score relative to the top-ranked pose was selected as the most reliable binding orientation. Protein–ligand interactions, including hydrogen, hydrophobic, and π–π interactions, were analyzed using Discovery Studio Visualizer (DSV) v2019. All docking experiments were performed under default Auto Dock Vina parameters except where specified.

### Extraction of leaves

Leaves of BL were collected, washed twice with tap water and once with double-distilled water to remove adhering dust and debris, and then shade-dried at room temperature (25–28°C) for 7–10 days. The dried leaves were pulverized into coarse powder using a mechanical grinder and sieved through a 40-mesh sieve. Approximately 250 g of powdered leaves were first subjected to defatting with petroleum ether (boiling point range: 60–80°C) in a Soxhlet apparatus for 8–10 cycles until the siphon solvent became colourless. The defatted material was then dried at room temperature to remove residual petroleum ether. The dried marc was subsequently extracted with 99% methanol using a soxhlet apparatus for 72 hr with continuous reflux, replacing fresh solvent every 8 hr to ensure complete extraction. In order to obtain a viscous, semi-solid crude extract, the methanolic extract was filtered through whatman No. 1 filter paper and concentrated under reduced pressure using a rotary evaporator (IKA RV 10) at 40°C. The extract was further dried in a vacuum desiccator to remove traces of solvent and stored at 4°C in an airtight container.[16]

## Animal grouping and design of study

Albino Wistar rats (Either sex, 180–200 g) were procured with an approval by the IAEC, Belagavi (Reg. No. 221/Re/S/CPCSEA/2000; Resolution No. 29). The animals were housed in solid-bottom polypropylene cages with stainless-steel grills and provided bedding of clean, dust-free paddy husk. They were maintained under standard laboratory conditions (ambient temperature, controlled humidity, and a 12 hr light/dark cycle) with free access to standard feed and water. After a 10-day acclimatization period, the animals were switched to a high-fat, high-fructose diet to induce metabolic alterations (48 days).

Randomly, 36 rats were divided into six groups, with six rats in each group.

Group I (Normal): Received standard pellets and distilled water for 10 weeks.

Group II (HFHF): Received standard pellets, 25% fructose in drinking water, and high-fat diet (3 ml/kg) until the end of the study.

Group III (PIO): Received standard pellets, high-fat diet (3 ml/kg) and 25% fructose for 6 weeks, followed by Pioglitazone (2.7 mg/kg/day, p.o.) for 28 days.

Group IV (BL 200): Received standard pellets, high-fat diet (3 ml/kg) and 25% fructose for 6 weeks, followed by BL leaves extract (200 mg/kg/day, p.o.) for 28 days.

Group V (BL 400): Received standard pellets, high-fat diet (3 ml/kg) and 25% fructose for 6 weeks, followed by BL leaves extract (400 mg/kg/day, p.o.) for 28 days.

Group VI (BL 800): Received standard pellets, high-fat diet (3 ml/kg) and 25% fructose for 6 weeks, followed by BL leaves extract (800 mg/kg/day, p.o.) for 28 days.

Simple randomization method was used for group allocation, with a total of 36 animals (N = 36) included in the study. The dose was selected based on reported toxicity studies; no mortality is showed amongst the treated animals during 14 days at a dose of 2000 mg/kg. Therefore, submaximal doses i.e., $1/10^{th}$, $1/5^{th}$, and $2/5^{th}$ of the Maximum Tolerated Dose of $LD_{50}$ were administered orally for 28 days to evaluate the dose dependent effect.[18]

## Induction of insulin resistance

IR was induced in Wistar albino rats (Either sex, weighing 180–200 g, aged 8–10 weeks) by oral administration of a high-fat emulsion in combination with a high sugar diet, following the protocol of Renuka *et al.*,[7,8] with minor modifications. The high-fat diet was made by combining Indian vanaspati ghee and coconut oil in a 3:1 (v/v) ratio. We took 75 mL of vanaspati ghee and 25 mL of coconut oil and made total volume 100 mL, it had gone for 2 weeks. The rats were given 3 mL/kg body weight of emulsion orally (per day). The rats were provided a high sugar diet that contained 25% fructose and was administered orally along with drinking water. High fat and high sugar died was given till 42 days. The induction of insulin resistance was confirmed by measuring Fasting Blood Glucose (FBG) levels after an overnight fast (12 hr). Rats with FBG levels ≥150 mg/dL were considered insulin-resistant and included in subsequent experiments. A total of 36 rats, 30 rats were subjected to insulin resistance induction, and 6 rats were maintained as a normal control group receiving a standard laboratory diet and distilled water only.

## Measurement and methods

### *Oral Glucose Tolerance Test (OGTT)*

Throughout the study, daily food and water intake were monitored for each cage, while body weights of individual rats were recorded weekly to assess metabolic changes. After 28 days of treatment, Fasting Blood Glucose (FBG) and Oral Glucose Tolerance Test (OGTT) were conducted. For the OGTT, animals were fasted overnight (12 hr) with free access to water. Baseline fasting glucose was determined at 0 min via tail vein sampling using a portable glucometer (Janaushadhi glucometer, Pradhan Mantri Bhartiya Janaushadhi Pariyojana, Government of India). Subsequently, rats received an oral glucose solution (2 g/kg body weight in distilled water) by gavage. Blood glucose concentrations were then measured at 30, 60, 90, and 120 min following glucose administration. The glucose tolerance of each animal was assessed by calculating the Area Under the Curve (AUC).[19]

## Sample collection for biochemical, *ex vivo*, and histological studies

At the end of the study period (day 76), all rats were fasted for 12 hr, anesthetized with ketamine (80 mg/kg, i.p.) and xylazine (10 mg/kg, i.p.), and euthanized by cervical dislocation. Whole blood was collected into heparinized tubes and centrifuged at 3000 rpm for 10 min at 4°C to separate plasma, which was stored at −20°C until biochemical analysis.

The liver and skeletal muscle tissues were excised immediately, rinsed with ice-cold saline, blotted, and homogenized in Phosphate Buffer Saline (PBS, 0.1 M, pH 7.4) using a Teflon-glass homogenizer. The homogenates were centrifuged at 2500 rpm for 10 min at 4°C, and the resulting supernatants were collected for biochemical assays (e.g., antioxidant enzymes, lipid peroxidation, glycogen estimation). For the glucose uptake study, the rat hemi-diaphragm was carefully excised, rinsed in Tyrode's buffer, and incubated with glucose solution (200 mg/dL) in the presence or absence of insulin, as per standard protocols. The liver and pancreas tissues were fixed in 10% neutral-buffered formalin for 48 hr, processed by standard paraffin embedding, sectioned at 5 µm thickness, and stained with Hematoxylin and Eosin (H&E) for histological evaluation.[20]

## Determination of rerum biochemical parameters

The separated plasma samples were used for the estimation of lipid profile and insulin levels. Commercially available diagnostic kits (YUCCA Diagnostics, Kagal, India) were used to determine: Total Cholesterol (TC) (enzymatic CHOD-PAP method), High-Density Lipoprotein Cholesterol (HDL-C) (precipitation method followed by enzymatic CHOD-PAP method), and Triglycerides (TG) (enzymatic GPO-PAP method).

All assays were performed according to the manufacturer's instructions using a UV-Visible spectrophotometer (Shimadzu UV-1800, Japan) at specified wavelengths (TC: 505 nm; TG: 510 nm; HDL-C: 546 nm). The levels of Very Low-Density Lipoproteins (VLDL-C) and Low-Density Lipoproteins (LDL-C) were calculated using Friedewald's formula:

$$\text{VLDL-C (mg/dl)} = \frac{TG\ (mg/dL)}{5}$$

$$\text{LDL-C (mg/dl)} = \text{TC} - (\text{HDL - C} + \text{VLDL - C})$$

Plasma insulin concentrations were determined using a sandwich ELISA technique with a commercial kit (GENLISA™ Rat Insulin ELISA Kit, Krishgen Biosystems, Mumbai, India) according to the manufacturer's instructions. The absorbance was measured at 450 nm with a microplate reader (Bio-Rad iMark™, USA), and insulin levels were quantified based on a standard curve generated from rat insulin standards.[21] The Homeostatic Model Assessment of Insulin Resistance (HOMA-IR) was calculated using the following formula:

$$\text{HOMA-IR} = \frac{\text{Fasting glucose (mg/dL)} \times \text{Fasting insulin (µU/mL)}}{405}$$

where fasting glucose values were obtained during OGTT measurements.

Serum tumor necrosis factor-alpha (TNF-α) levels were quantified with a commercial ELISA kit (GENLISA™ Rat TNF-α ELISA, Krishgen Biosystems, Mumbai, India) following the manufacturer's instructions. Absorbance was read at 450 nm using a microplate reader, and concentrations were calculated from the corresponding standard curve.

## Determination of glycogen content, oxidative Stress biomarkers and glucose uptake

The collected liver and skeletal muscle supernatants were used for the estimation of glycogen content and oxidative stress biomarkers.

## Glycogen content

Glycogen was quantified by the anthrone method.[22] Briefly, 0.5 mL of tissue supernatant was mixed with 5 mL of anthrone reagent (0.2% anthrone in concentrated sulfuric acid), heated in a boiling water bath for 10 min, and rapidly cooled on ice. The absorbance was recorded at 620 nm using a UV-Visible spectrophotometer (Shimadzu UV-1800, Japan). Glycogen content was calculated using a standard calibration curve prepared with D-glucose and expressed as mg glycogen/g wet tissue.

## Oxidative stress biomarkers

The following antioxidant biomarkers were analyzed in tissue homogenates:

**Catalase (CAT)** activity was assessed using the colorimetric method of Aebi,[23] which measures the rate of Hydrogen Peroxide ($H_2O_2$) decomposition at 240 nm. Enzyme activity was expressed as units per milligram of protein (U/mg protein). Reduced Glutathione (GSH) content was estimated following the method of Ellman[24] using 5,5'-dithiobis-(2-nitrobenzoic acid) (DTNB) as the reagent. The formation of a yellow-colored chromophore was recorded at 412 nm, and results were expressed as micromoles of GSH per milligram of protein (µmol/mg protein).

**Superoxide Dismutase (SOD)** activity was measured using the pyrogallol auto-oxidation method,[25] where the inhibition of pyrogallol oxidation was recorded at 420 nm. Enzyme activity was expressed as units per milligram of protein (U/mg protein).

## Glucose uptake in rat hemi-diaphragm

Glucose uptake was evaluated following the method of Kulkarni and Aiman (1958), with minor modifications as outlined by Chattopadhyay *et al.*,[26] In brief, hemi-diaphragms were isolated from overnight-fasted rats, rinsed with Tyrode's buffer, and incubated at 37°C for 30 min in flasks containing 2 mL of glucose solution (200 mg/dL), either in the presence or absence of insulin (0.25 IU/mL). Following incubation, the residual glucose concentration in the medium was determined using the Glucose Oxidase–Peroxidase (GOD-POD) method, with absorbance measured at 505 nm. The percentage of glucose uptake was calculated using the formula:

$$\text{Glucose Uptake (\%)} = \frac{Initial\ glucose\ content - Final\ glucose\ content}{Initial\ glucose\ content}\ X\ 100$$

## Histopathological analysis of the liver and pancreas

The excised liver and pancreas tissues were immediately rinsed in ice-cold phosphate buffer saline (PBS, pH 7.2) to remove adhering blood and clots. The tissues were then immersed in 10% neutral-buffered formalin and kept at room temperature for 24-48 hr to achieve optimal fixation. After fixation, the specimens underwent routine paraffin embedding. This involved sequential dehydration in graded ethanol concentrations (70%, 80%, 90%, and 100%), clearing with xylene, and infiltration with molten paraffin wax maintained at 58-60°C. Paraffin blocks were prepared, and thin tissue sections (4–5 µm) were cut using a rotary microtome. The sections were placed on glass slides, deparaffinized with xylene, rehydrated through descending ethanol grades, and stained with Hematoxylin and Eosin (H&E) using standard procedures. The stained tissues were examined

under a light microscope (Olympus CX43, Japan) at 100× and 400× magnifications to assess histopathological alterations. Changes in hepatocytes, central vein, sinusoidal architecture, pancreatic acini, and islets of Langerhans were carefully documented, and differences between control and experimental groups were compared. Representative micrographs were captured using a digital imaging system for record-keeping. Representative photomicrographs were captured using a digital camera attachment for documentation.

## Histopathological analysis of liver and pancreas

The data has been expressed in "Mean±SEM" "($n$=6 or 3)" and analyzed by one-way ANOVA or two-way ANOVA followed by Bonferroni's multiple comparison test by Graph Pad Prism 9.1.2. $p$"<"0.05" was consider as statistically significant."

**Table 1: Thirty-three insulin resistance-related targets of *Buchanania lanzan* leaves.**

| Sl. No. | Target Name | Uniprot ID | Gene Name |
|---|---|---|---|
| 1. | Adrenoceptor Beta 2 | P07550 | ADRB2 |
| 2. | AKT Serine/Threonine Kinase 1 | P31749 | AKT1 |
| 3. | Alpha-glucosidase | P10253 | GAA |
| 4. | Androgen Receptor | P10275 | AR |
| 5. | ATP Binding Cassette Subfamily G Member 2 | Q9UNQ0 | ABCG2 |
| 6. | Dipeptidyl Peptidase 4 | P27487 | DPP4 |
| 7. | Epidermal Growth Factor Receptor | P00533 | EGFR |
| 8. | Estrogen Receptor 1 | P03372 | ESR1 |
| 9. | Fatty Acid Binding Protein 4 | P15090 | FABP4 |
| 10. | Glucagon-Like Peptide 1 Receptor | P43220 | GLP1R |
| 11. | Glucagon Receptor | P47871 | GCGR |
| 12. | Glycogen Synthase Kinase 3 Beta | P49841 | GSK3B |
| 13. | Hypoxia Inducible Factor 1 Subunit Alpha | Q16665 | HIF1A |
| 14. | Insulin-Like Growth Factor 1 | P05019 | IGF1 |
| 15. | Insulin-Like Growth Factor Binding Protein 1 | P08833 | IGFBP1 |
| 16. | Insulin-Like Growth Factor Binding Protein 3 | P17936 | IGFBP3 |
| 17. | Insulin Receptor | P06213 | INSR |
| 18. | Insulin Receptor Substrate 2 | Q9Y4H2 | IRS2 |
| 19. | Interleukin 2 | P60568 | IL2 |
| 20. | Interleukin 6 | P05231 | IL6 |
| 21. | Mechanistic Target of Rapamycin Kinase | P42345 | MTOR |
| 22. | Mitogen-Activated Protein Kinase 1 | P28482 | MAPK1 |
| 23. | Mitogen-Activated Protein Kinase 10 | P53779 | MAPK10 |
| 24. | Mitogen-Activated Protein Kinase 14 | Q16539 | MAPK14 |
| 25. | Nitric Oxide Synthase 2 | P35228 | NOS2 |
| 26. | Peroxisome Proliferator-Activated Receptor Alpha | Q07869 | PPARA |
| 27. | Peroxisome Proliferator-Activated Receptor Gamma | P37231 | PPARG |
| 28. | Protein Kinase C Alpha | Q9NRD5 | PRKCA |
| 29. | Protein Tyrosine Phosphatase Non-receptor Type 1 | P18031 | PTPN1 |
| 30. | Resistin | Q9HD89 | RETN |
| 31. | Toll-Like Receptor 2 | O60603 | TLR2 |
| 32. | Tumor Necrosis Factor | P01375 | TNF |
| 33. | Vascular Endothelial Growth Factor A | P15692 | VEGFA |

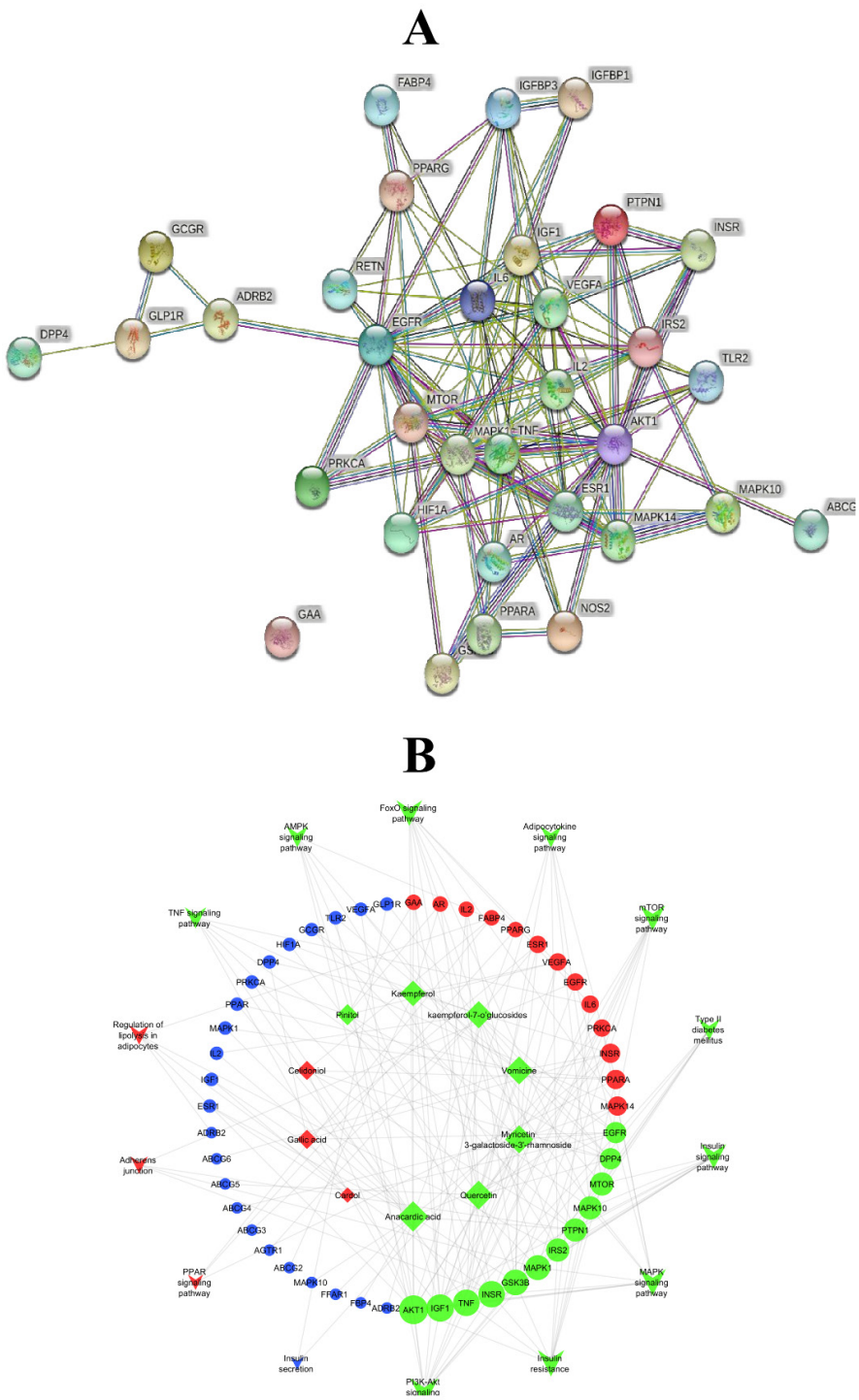


**Figure 1:** A) Protein-protein interaction network B) Network interaction of pathways, protein molecules, and phytoconstituents. In the network interaction, the node with the higher edge is represented with green color, which gradually decreases to blue.

## RESULTS

### Enrichment and network analysis

To identify the pathways that are modulated by the phytoconstituents, gene set enrichment analysis was performed on the set of proteins associated in IR. Among them, 14 pathways were significantly enriched for IR and associated complications pathways. The PI3K-Akt signaling pathway scored the highest edge count of 12 and the lowest FDR value of 8.33E-12 via modulating MAPK1, IL2, TLR2, EGFR, IGF1, INSR, GSK3B, MTOR, IL6,

PRKCA, AKT1, and VEGFA. Similarly, insulin resistance and MAPK signaling pathway scored the second-highest edge count of 10. Table 2 summarizes the 14 molecular pathways modulated by phytocompounds.

Compound, protein, pathways connection network contains 182 edges and 57 nodes (Figure 1 A). Among 57 nodes, 10 were phytoconstituents, 33 protein targets, and 14 molecular pathways. Among 10 compounds, anacardic acid scored the highest edge count i.e., 15, via targeting 15 protein molecules i.e., INSR, IGF1, MAPK1, EGFR, GSK3B, PTPN1, PRKCA, ESR1, IL2, FABP4, PPARG, PPAR, ADRB2, MAPK10, and FFAR1. Similarly, among 14 pathways, the PI3K-Akt signaling pathway scored the highest edge count that includes 12 protein molecules i.e., INSR, IGF1, Akt1, MAPK1, EGFR, GSK3B, mTOR, VEGFA, PRKCA, IL2, IL6, and TLR2. (Figure 1 B).

## Docking analysis

Based on the current therapeutic drug targets for DM, we selected phytocompounds predicted for three essential protein targets i.e., DPP4, PPARG, and PTPN1 for molecular docking analysis. Among the selected compounds, Myricetin 3-galactoside-3'-rhamnoside, kaempferol-7-o'glucoside, and quercetin were found to be the best hits for PPARG via scoring lowest BE of -8.9, -8.3, -7.6 kcal/mol and via forming a maximum number of interactions with active site residues i.e., 8, 7, 7 respectively compared to standard molecule Pioglitazone that scored lowest BE of -8.3 and 7 interactions with active site residues (Figure 2A and 2D).

Myricetin 3-galactoside-3'-rhamnoside, kaempferol-7-O'glucoside, and quercetin formed common four interactions with amino acid residues of PPARG i.e., Ile262, Arg280, Arg288, Ile341. Further, kaempferol-7-o'glucoside, quercetin, and gallic acid were found to be the best hits against DPP4. These three compounds scored the lowest BE of -8.5, -7.9, and -6.4 kcal/mol and formed 7, 7, 7 interactions with active site residues of DPP4 respectively. However, kaempferol, pinitol, and vomicine were also found to be the next best hits. A standard molecule Sitagliptin scored the lowest BE of -8.7 kcal/mol and formed 6 interactions with active site residues (Figure 2B and 2E).

Myricetin 3-galactoside-3'-rhamnoside, kaempferol-7-o'glucoside, and kaempferol were found to be the best hit against PTPN1 which scored the lowest BE of -7.6, -8, -7.5 kcal/mol and formed 6, 5, and 5 interactions with active site residues of the PTPN1 (Figure 2C and 2F). Whereas, standard molecule 4-[3-(dibenzylamino) phenyl]-2,4-dioxobutanoic acid showed 8 interactions with active site residues at -7.1kcal/mol BE. Detailed results are reported in Table 3.

**Table 2: Gene set Enrichment analysis of proteins involved in insulin resistance.**

| KEGG pathway ID | Pathway description | Gene count | FDR | Genes within pathway |
|---|---|---|---|---|
| hsa04151 | PI3K-Akt signaling pathway | 12 | 8.33E-12 | MAPK1,IL2,TLR2,EGFR,IGF1,INSR,GSK3B,MTOR,IL6,PRKCA,AKT1,VEGFA |
| hsa04931 | Insulin resistance | 10 | 1.51E-13 | INSR,GSK3B,MAPK10,MTOR,PTPN1,IRS2,PPARA,IL6,TNF,AKT1 |
| hsa04010 | MAPK signaling pathway | 10 | 7.16E-10 | MAPK1,MAPK14,EGFR,IGF1,INSR,MAPK10,TNF,PRKCA,AKT1,VEGFA |
| hsa04068 | FoxOsignaling pathway | 9 | 2.76E-11 | MAPK1,MAPK14,EGFR,IGF1,INSR,MAPK10,IRS2,IL6,AKT1 |
| hsa04910 | Insulin signaling pathway | 8 | 9.34E-10 | MAPK1,INSR,GSK3B,MAPK10,MTOR,PTPN1,IRS2,AKT1 |
| hsa04150 | mTORsignaling pathway | 8 | 1.75E-09 | MAPK1,IGF1,INSR,GSK3B,MTOR,TNF,PRKCA,AKT1 |
| hsa04920 | Adipocytokinesignaling pathway | 6 | 1.54E-08 | MAPK10,MTOR,IRS2,PPARA,TNF,AKT1 |
| hsa04668 | TNF signaling pathway | 6 | 1.45E-07 | MAPK1,MAPK14,MAPK10,IL6,TNF,AKT1 |
| hsa04152 | AMPK signaling pathway | 6 | 2.47E-07 | PPARG,IGF1,INSR,MTOR,IRS2,AKT1 |
| hsa04930 | Type II diabetes mellitus | 6 | 2.70E-09 | MAPK1,INSR,MAPK10,MTOR,IRS2,TNF |
| hsa04923 | Regulation of lipolysis in adipocytes | 5 | 1.82E-07 | FABP4,INSR,ADRB2,IRS2,AKT1 |
| hsa04520 | Adherens junction | 4 | 1.87E-05 | MAPK1,EGFR,INSR,PTPN1 |
| hsa03320 | PPAR signaling pathway | 3 | 0.00049 | FABP4,PPARG,PPARA |
| hsa04911 | Insulin secretion | 2 | 0.0128 | GLP1R,PRKCA |

## Effect of HFHF diet and various treatments on water intake, Body Weight (BW), and food intake

Figure 3 revealed that, the BW is examined weekly and compared at the end of the ten weeks. HFHF group showed highly significant increase in BW (325.1±13.40) compared to normal control group (248.7±2.462) (Figure 3A). Group treated with PIO showed slightly increase in BW at the completion of 10$^{th}$ week, while BL 800 group decrease BW at the termination of 10$^{th}$ week compared to initial treatment week 7. Food (Figure 3B) and water intake (Figure 3C) are considerably higher in the HFHF group ($p$<0.001) than in the normal control group till the end of week 10.

## Effect of HFHF and BL extract on fasting insulin level and FBG level.

There was significantly ($p$<0.001) increase in fasting blood glucose level plus fasting insulin levels has been seen in HFHF treated groups (144.7±3.180, 47.09±3.115) in comparison with normal control group (82.67±1.764, 4.07±1.443). The treatment with BL extract lowered both glucose as well as insulin level as associated to disease control group (Figure 3D, Figure 4B).

## Effect of HFHF and BL extract on insulin sensitivity

OGTT revealed, in association to the normal control group, the AUC of glucose in disease control group increased significantly ($p$<0.001) (Figure 3D and 3F). And which was significantly ($p$<0.01) decreased in PIO, and dose-dependent decline in total area under curve in BL 200, BL 400 and BL 800 groups, compared to normal control group. Insulin sensitivity is confirmed by HOMA-IR (Figure 4A). Less HOMA-IR value indicates more insulin sensitivity. The values of it are represented in Figure 4A. Normal control group (0.6895±0.2537) is shown statistically significant change ($p$<0.001) in insulin sensitivity associated to disease control group (16.8±1.018). Group treated with PIO (2.085±0.314) exhibited more insulin sensitivity than BL 800 (3.590±0.569) treated group.

## Effect of HFHF and BL extract on lipid profile

As depicted in Table 4, the disease control group demonstrated a significant ($p$<0.001) rise in TG, TC, LDL, and VLDL and significant ($p$<0.001) reduction in HDL when associated to the normal control group. All of the treatments reversed these changes. The BL treated groups had a significant ($p$<0.001) rise in HDL and a significant ($p$<0.001) reduction in TG, TC, LDL, and VLDL when related to the disease control group.

## Effect of HFHF and BL extract on serum TNF-α level

Normal control group (4.42±1.424) is shown statistically considerable difference ($p$<0.05) in insulin sensitivity associated with disease control group (17.56±5.489). BL 400 and BL 800 groups (11.64±2.648, 6.93±3.009) showed decrease in TNF-α level in compared with the disease control group but the difference is not statistically significant (Figure 4F).

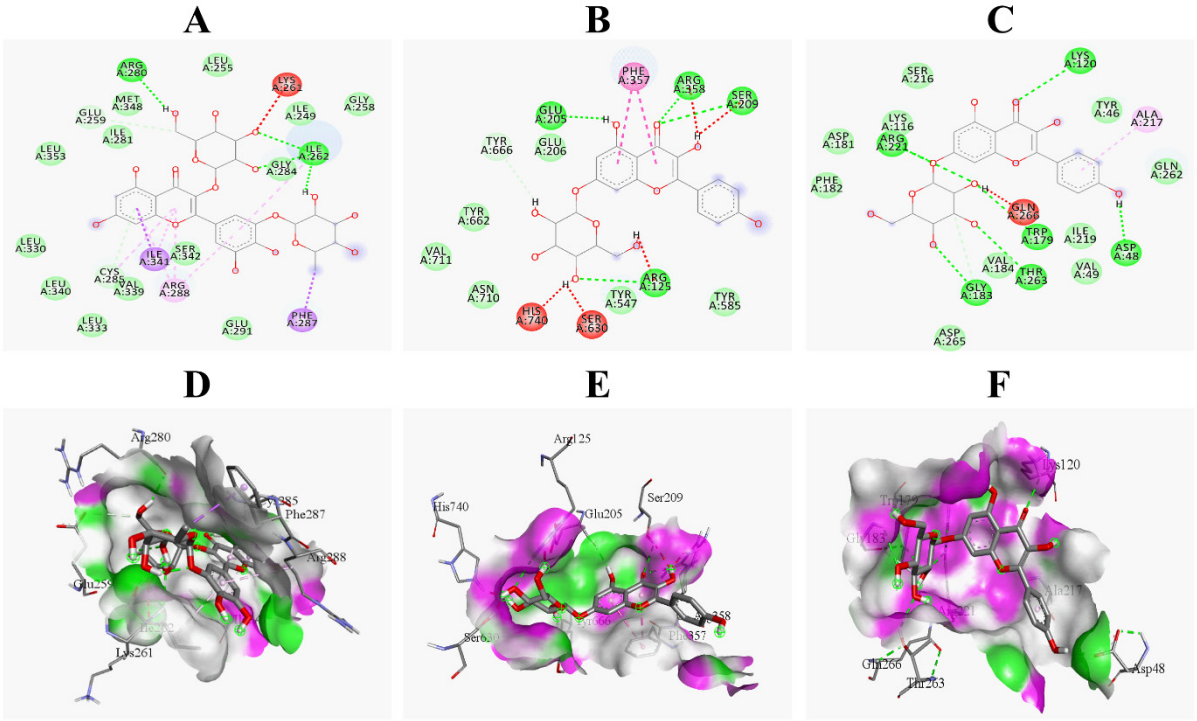


**Figure 2:** 2D interactions Binding energies of compounds A) PPARG-Myricetin 3-galactoside-3'-rhamnoside C) DPP4-Kaempferol-7-O-glucoside E) PTPN1-Kaempferol-7-O-glucoside; 3D interactions/3D pose binding energies of compounds B) PPARG-Myricetin 3-galactoside-3'-rhamnoside D) DPP4-Kaempferol-7-O-glucoside F) PTPN1-Kaempferol-7-O-glucoside.

**Table 3: Binding energies and proteins associated with the interaction of targets and phytoconstituents.**

| Target | Compound | BE (Kcal/mol) | Conventional HBI | Non-conventional interactions | No. of HBI | No. of non-Conventional interactions | No. of interaction with active site recidues |
|---|---|---|---|---|---|---|---|
| PPARG | Gallic acid | -5.2 | His425,Leu421,Phe432 | Lys422 | 3 | 1 | 0 |
| | Kaempferol | -7.3 | Ser342 | Ile281,Ile341,Cys285,Arg288 | 1 | 4 | 5 |
| | Kaempferol-7-o'glucosides | -8.3 | Glu291,Glu259,Arg280,Ser342 | Arg288,Ile262,Ile341 | 4 | 3 | 7 |
| | Myricetin 3-galactoside-3'-rhamnoside | -8.9 | Arg280,Ile262 | Glu259,Lys261,Phe287,Arg288, Ile341,Cys285 | 2 | 6 | 8 |
| | Pinitol | -5.4 | Arg433 | - | 1 | 0 | 0 |
| | Quercetin | -7.6 | Ser342,Ile262,Arg280 | Arg288,Ile281,Ile341,Gly284, Cys285 | 3 | 5 | 7 |
| | Vomicine | -9.2 | Met463 | Leu465,Lys457 | 1 | 2 | 3 |
| | Pioglitazone | -8.3 | Cys285 | Arg288,Leu330,Tyr473,Leu469, Leu465,Leu453,Gly469 | 1 | 7 | 7 |
| DPP4 | Gallic acid | -6.4 | Thy351,Ser349,Arg382,Glu347 | Val354,Gly355,Ser376 | 4 | 3 | 7 |
| | Kaempferol | -8.1 | Asn562,Gln527,Lys512 | Pro510,Ile529,Phe559,Arg560 | 3 | 4 | 5 |
| | Kaempferol-7-o'glucosides | -8.5 | Arg358,Ser209,Glu205,Arg125 | Phe357,His740,Ser630 | 4 | 3 | 7 |
| | Myricetin 3-galactoside-3'-rhamnoside | -8.8 | Ala306,Leu410,Ser462 | Ala409,Ala465,Pro218,Pro159,His363 | 3 | 5 | 0 |
| | Pinitol | -5.6 | Thy350,Ser376,Asn377 | Met348,Glu378 | 3 | 2 | 5 |
| | Quercetin | -7.9 | Arg358,Ser630,Arg125,Asn710,Glu206 | Tyr662,Phe357 | 5 | 2 | 7 |
| | Vomicine | -8.9 | Lys554,Tyr752 | Trp629,Trp627 | 2 | 2 | 4 |
| | Sitagliptin | -8.7 | Gly355,Thy351,Glu378,Lys589,Trp352,Arg382, | Val354,Glu347,Met348,Glu379 | 6 | 4 | 6 |
| PTPN1 | Gallic acid | -5.5 | Ser50,Arg47,Leu37 | Lys36,Asn44,Typ46 | 3 | 2 | 1 |
| | Kaempferol | -7.5 | Arg221,Asp181,Gly183,Ser216 | Thy263 | 4 | 1 | 5 |
| | Kaempferol-7-o'glucosides | -8 | Lys120,Arg221,Gly183,Thy263,Trp179,Asp48 | Ala217,Gly183,Gln266 | 6 | 2 | 5 |
| | Myricetin 3-galactoside-3'-rhamnoside | -7.6 | Glu115,Ser216,Trp179,Thr263,Gln266,Arg221 | Asp48,Ala217 | 6 | 1 | 6 |
| | Pinitol | -5.4 | Gly183,Trp179,Gln266 | Trp179,Gly183 | 3 | 2 | 4 |
| | Quercetin | -7.4 | Arg221 | Thy263 | 1 | 1 | 2 |
| | Vomicine | -8.2 | Ser216 | Ala217,Cys215 | 1 | 2 | 3 |
| | 4-[3-(dibenzylamino) phenyl]-2,4-dioxobutanoic acid | -7.1 | Gly183,Trp179,Pro180,Asp181,Arg221 | Tyr46,Ala217,Lys120 | 5 | 3 | 8 |

## Effect of HFHF and BL extract on glycogen level in liver and skeletal muscle

As shown in Figure 4D and 4E, the glycogen in the liver and skeletal muscle was significantly ($p$<0.001) lower into the disease control group. (12.56±0.4406 and 6.747±0.3671) as compared to normal control group (43.47±1.395 and 14.15±0.3486 respectively). There was significantly ($p$<0.001) increase in stored glycogen of the skeletal muscle into PIO (12.80±0.3655), BL 400 (9.406±0.3708) and BL 800 (10.72±0.5996) treated groups compared to disease control group (6.747±0.3671). Similarly, a significant ($p$<0.001) rise in liver glycogen was seen in PIO (39.17±0.4664), BL 400 (19.68±0.9751) and BL 800 (30.60±0.6167) groups in comparison with disease control group (12.56±0.4406).

## Effect of HFHF and BL extract on glucose uptake

After treatment of 28 days, in comparison to the normal group (70.41±1.523), the disease control (15.59±0.6310) group's percentage of glucose uptake was considerably ($p$<0.001) lower (Figure 4C). Similarly, PIO treatment groups (58.37±1.370), had a significant ($p$<0.001) increase in percent glucose uptake comparison to disease control group (15.59±0.6310), also BL 800 treated group showed significant increase (46.79±1.811) in glucose uptake, compared to disease control group (15.59±0.6310).

## Effect of HFHF and BL extract on oxidative imbalance

HFHF induced (disease control group) insulin resistance rats (SOD-0.1085±0.002 and CAT-1.046±0.22) exhibited significantly ($p$<0.001) decrease in GSH, SOD as well as CAT levels related to normal control group (5.897±0.5627, 0.2904±0.003 and 7.423±1.323 respectively) (Table 5). Treatment with BL 800 (9.364±0.8334, 0.2189±0.004, 6.27±0.6788) exhibited good antioxidant capacity in comparison with BL 200 (6.44±0.3744, 0.215±0.002, 3.452±0.617) and BL 400 (9.707±0.6267, 0.2182±0.009, 4.578±0.317) (Table 5).

## Effect of HFHF and BL extract on liver histology

HFHF treated group bared highest degree of venous congestion, least degree of inflammation, and, ballooning degeneration compared to normal control group. The least degree of venous congestion is seen in PIO treated group and it repaired ballooning

**Table 4: Effect of BL extract on serum levels of HDL, LDL, TG, VLDL, and TC in HFHF induced insulin resistance rats.**

| Group | HDL (mg/dL) | LDL (mg/dL) | TG (mg/dL) | VLDL (mg/dL) | TC (mg/dL) |
|---|---|---|---|---|---|
| Group I (NORMAL) | 48.28±1.889 | 37.15±3.006 | 68.76±2.401 | 13.75±0.4803 | 99.18±1.752 |
| Group II (HFHF) | 20.55±0.5546$^{*}$ | 110.3±1.553$^{*}$ | 112.5±3.062$^{*}$ | 22.5±0.6125$^{*}$ | 153.3±1.217$^{*}$ |
| Group III (PIO) | 42.94±1.811$^{\#}$ | 51.93±3.302$^{\#}$ | 73.59±1.838$^{\#}$ | 14.72±0.3677$^{\#}$ | 109.6±2.184$^{\#}$ |
| Group IV (BL 200) | 23.27±0.7057$^{\#@}$ | 97.68±3.011$^{\#\#\#@}$ | 107.7±1.586$^{@}$ | 21.54±0.3173$^{@}$ | 143.5±2.201$^{\#\#@}$ |
| Group V (BL 400) | 30.75±1.389$^{\#@\$\$\$}$ | 81.45±2.118$^{\#@\$\$}$ | 103.6±1.631$^{@}$ | 20.71±0.3262$^{@}$ | 132.9±1.562$^{\#@\$\$}$ |
| Group VI (BL 800) | 36.11±1.797$^{\#@@@\$}$ | 59.31±1.151$^{\#\$\%}$ | 95.76±1.105$^{\#@\$\$}$ | 19.15±0.2210$^{\#@\$\$}$ | 115.8±1.746$^{\#\$\%}$ |

$^{*}p$<0.001 vs. Normal group; $^{\#}p$<0.001, $^{\#\#}p$<0.01, $^{\#\#\#}p$<0.05 vs. HFHF group; $^{@}p$<0.001 vs. PIO group, $^{\$}p$<0.001, $^{\$\$}p$<0.01, $^{\$\$\$}p$<0.05 vs. BL 200 group; $^{\%}p$<0.001 vs. BL 400 group.

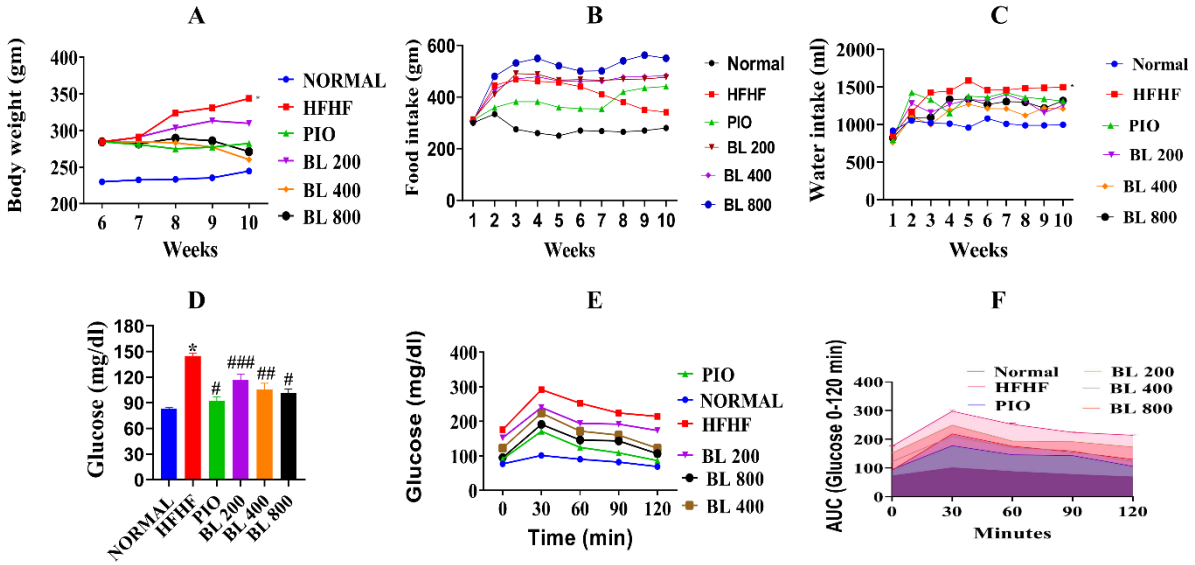


**Figure 3:** Effect of various treatments on (A) Body weight, (B) Food intake and (C) Water intake of IR rats. *$p$<0.001 vs. Normal group. Effect of HFHF and BL extract on (OGTT) oral glucose tolerance test. D) Fasting blood glucose level. E) Glucose level at 30 min interval during oral glucose tolerance test; F) Total area under curve of glucose. *$p$<0.001 vs. Normal group; $^{\#}p$<0.001, $^{\#\#}p$<0.01, $^{\#\#\#}p$<0.05 vs. HFHF group.

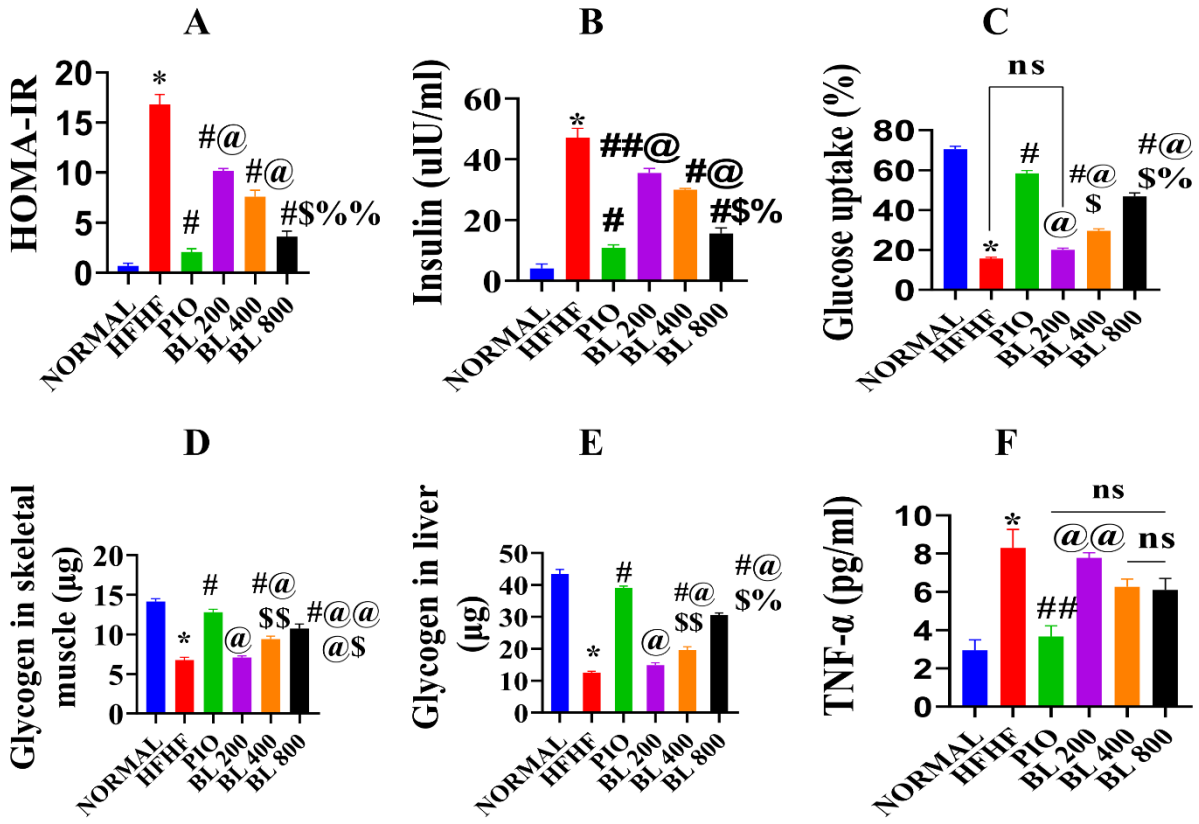


**Figure 4:** Effect BL extract on fasting insulin level and HOMA-IR. A) HOMA-IR level B) Fasting insulin level. C) Effect of BL extract on glucose uptake.. Effect of BL extract on glycogen level in D) Skeletal muscle and E) Liver. F) Effect of HFHF and BL extract on serum TNF-α. $^{*}p<0.001$ vs. Normal group; $^{\#}p<0.001$, $^{\#\#}p<0.01$ vs. HFHF group; $^{@}p<0.001$, $^{@@}p<0.01$, $^{@@@}p<0.05$ vs. PIO group, $^{\$}p<0.001$ vs. BL 200 group; $^{\%}p<0.001$, $^{\%\%}p<0.01$ vs. BL 400 group.

degeneration and inflammatory damage. Among three doses, BL 800 recovered inflammatory damage but failed to recover venous congestion and ballooning degeneration compared to PIO treated group (Figure 5 and Table 6).

## Effect of HFHF and BL extract on histology of pancreas

Figure 6 Revealed that, there is significantly ($p<0.001$) increase in average size of β-cells and length of islet in disease control group (34.40±2.386, 346.7±30.87) as compared to normal control group (11.20± 0.6110, 64.97±7.620). The groups treated with PIO, BL 400, and BL 800 saved the normal morphology of islets and β-cells as compared to disease control group (Figures 6 and 7).

## DISCUSSION

The current study evaluated the anti-insulin resistance (anti-IR) activity of BL leaves and explored the underlying mechanisms through *in silico* and *in vivo* methods. HFHF-induced obesity and its associated IR led to metabolic alterations, including weight gain, disrupted glucose homeostasis, and inflammatory states.[28] Treatment with BL extract improved physical parameters, such as body weight, food, and water intake, in HFHF-induced IR rats (Figure 3). This is consistent with the traditional use of BL leaves as a thirst quencher.[27,28] Furthermore, the observed reductions in food intake may correlate with DPP4 modulation by BL, which influences appetite control via glucagon-like peptide-1 (GLP-1) signaling.[29]

PTP1B overexpression is a hallmark of IR as it impairs insulin receptor signaling, reducing glucose uptake in tissues.[30,31] In this study, BL-treated rats demonstrated increased glycogen levels in the liver and skeletal muscles (Figure 4D and Figure 4E), suggesting that BL may modulate PTP1B activity, restoring insulin signaling and glucose metabolism. This aligns with findings showing that inhibiting PTP1B improves insulin sensitivity and glycogen synthesis.[32] Histopathological analysis further showed that BL treatment reduced β-cell hypertrophy and islet enlargement, commonly observed in IR and diabetic states, suggesting a protective role of BL in pancreatic function.[33,34]

The activation of PPARG is crucial for improving insulin sensitivity by regulating glucose metabolism genes.[35] BL treatment improved glucose tolerance and HOMA-IR values, showing a comparable effect to Pioglitazone (PIO) (Figure 4A). *In silico*

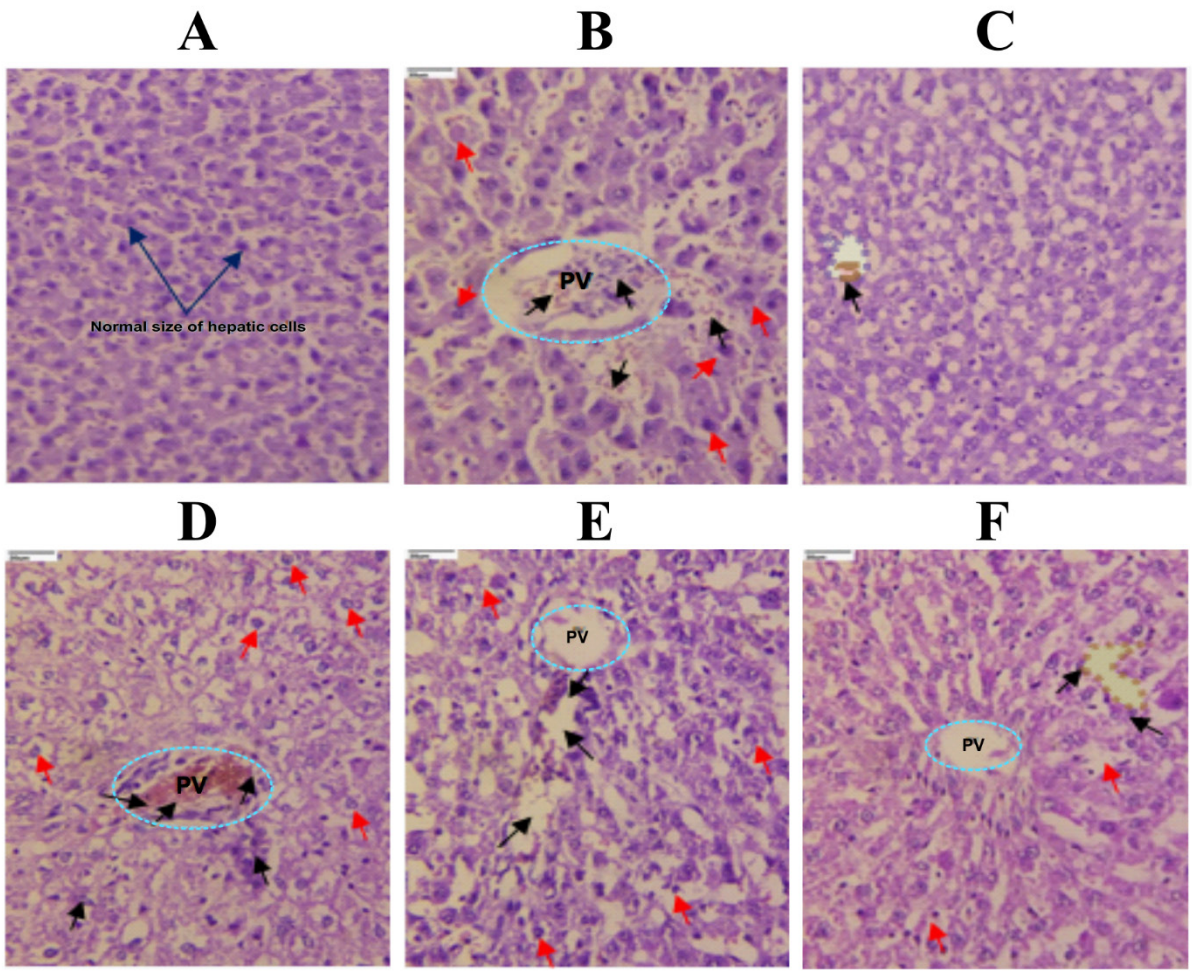


**Figure 5:** Histological changes in liver. A) Normal, B) Disease control, C) PIO, D) BL 200, E) BL 400, F) BL 800.

**Table 5: Effect of HFHF and BL on oxidative imbalance.**

| Groups | SOD (unit/mg protein) | Catalase (U/min.mg of protein) | GSH (µMol/mg of protein) |
|---|---|---|---|
| Group I (NORMAL) | 0.2803±0.01682 | 7.423±1.323 | 14.91±0.303 |
| Group II (HFHF) | 0.1085±0.02559* | 1.046±0.2272* | 5.897±0.5627* |
| Group III (PIO) | 0.2543±0.019## | 5.921±0.9017## | 11.91±0.3418# |
| Group IV (BL 200) | 0.1112±0.02315@@ | 3.452±0.6176 | 6.44±0.3744@ |
| Group V (BL 400) | 0.1976±0.02667 | 4.578±0.3171# | 9.707±0.6267#$$ |
| Group VI (BL 800) | 0.2291±0.02831###$$$ | 6.27±0.6788### | 9.364±0.8334##@@@$$ |

*$p<0.001$ vs. Normal group; $^{\#}p<0.001$, $^{\#\#}p<0.01$, $^{\#\#\#}p<0.05$ vs. HFHF group; $^{@}p<0.001$,; $^{@@}p<0.01$, $^{@@@}p<0.05$ vs. PIO group, $^{\$}p<0.001$, $^{\$\$}p<0.01$, $^{\$\$\$}p<0.05$ vs. BL 200 group.

**Table 6: Histological changes in the liver.**

| | Group I (Normal) A | Group II (Disease control) B | Group III (PIO) C | Group IV (BL 200) D | Group V (BL 400) E | Group VI (BL 800) F |
|---|---|---|---|---|---|---|
| Venous congestion | - | ++ | + | ++ | ++ | + |
| Ballooning degeneration | - | ++ | - | ++ | ++ | + |

Note: ++ signify "highest degree of damage", + denote "least degree of damage" and - signify "total repair".

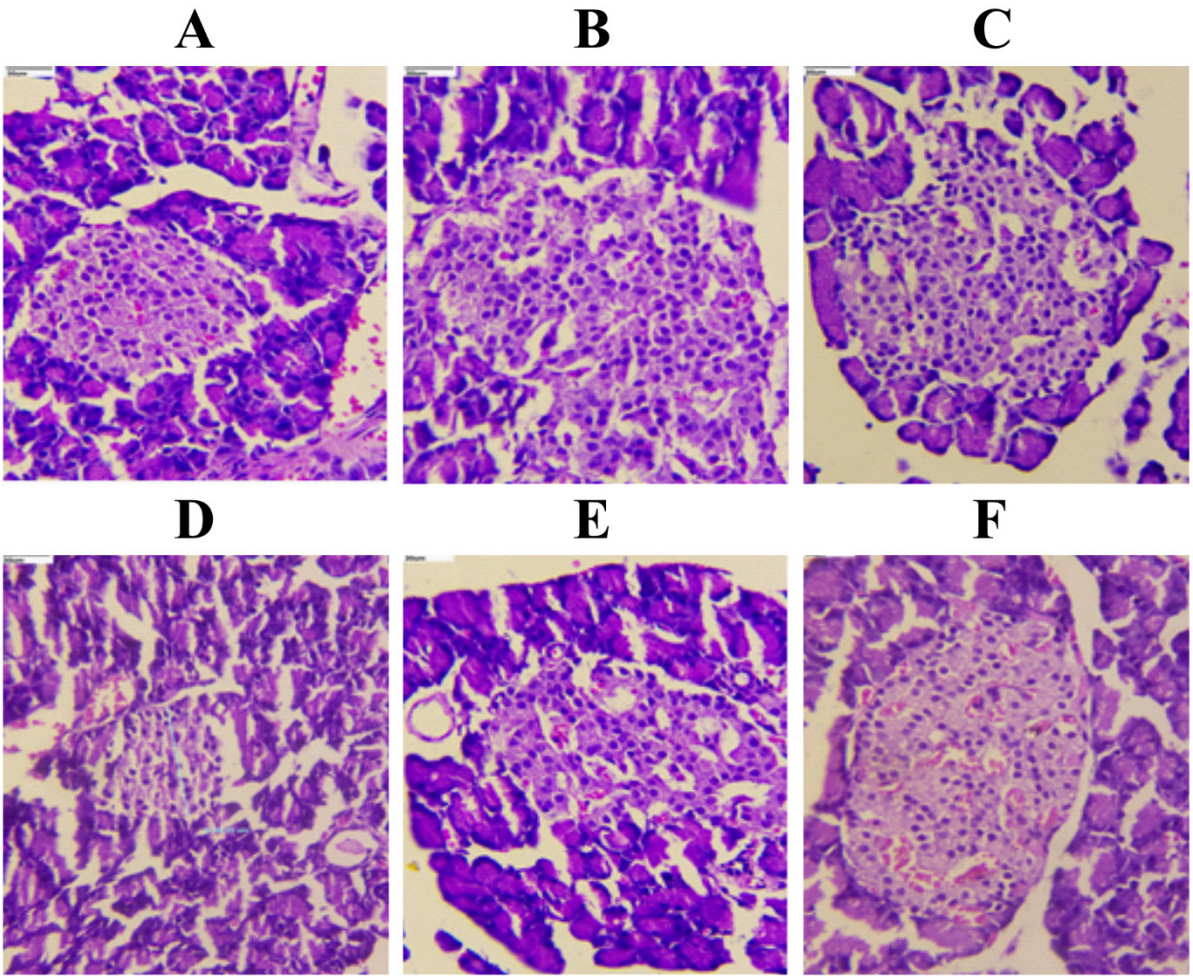


**Figure 6:** Histological changes in pancreas. A) Normal, B) Disease control, C) PIO, D) BL 200, E) BL 400, F) BL 800.

docking revealed that myricetin 3-galactoside-3'-rhamnoside, kaempferol-7-o'-glucoside, and quercetin exhibited strong interactions with PPARG, supporting the hypothesis that these flavonoids may act as PPARG activators. The improved glucose uptake, glycogen synthesis in liver and skeletal muscles observed in vivo suggest a potential stimulatory effect of BL on PPARG, similar to PIO.[36,37]

Currently diet-induced insulin resistance model, BL treatment improved glycemic control and insulin sensitivity alongside meaningful antioxidant gains (↑SOD, ↑GSH; ↓lipid peroxidation). While Pioglitazone (PIO), a Thiazolidinedione (TZD),[38] is an established insulin sensitizer via PPARG agonism, the BL appears to leverage multi-target, synergistic mechanisms that extend beyond a single nuclear receptor pathway and may carry a more favorable side-effect profile at the effective doses tested.[39-42]

Unlike pioglitazone, which acts mainly via PPARG and has notable side effects, BL exerts multi-targeted actions contributing to improved insulin sensitivity,[43] synergistic insulin-sensitizing effects anchored in antioxidant,[44] and anti-inflammatory actions,[45] with signals of a gentler side-effect profile in the present model,[46,47] These attributes suggest BL as a promising adjunct or alternative for insulin resistance,[48] pending rigorous standardization, pharmacology, and clinical validation.[49]

HFHF diets disrupt the PI3K-Akt signaling pathway by upregulating Diacylglycerol (DAG) levels and activating PKC, leading to reduced GLUT4 translocation and impaired glucose metabolism.[49] BL treatment improved lipid profiles, glucose uptake, and glycogen storage, indicating reactivation of PI3K-Akt signaling. *In silico* findings further supported these observations, demonstrating that BL's phytoconstituents target this pathway, thereby restoring metabolic homeostasis (Figure 4D and 4E).[50]

BL's anti-inflammatory and antioxidant activities significantly contribute to its anti-IR effects. Elevated TNF-α levels in IR disrupt insulin signaling and glucose uptake in tissues.[51] BL extract significantly reduced TNF-α levels. (Figure 4F), correlating with improved insulin signaling and glucose metabolism. Additionally, BL enhanced antioxidant enzyme activities (GSH, CAT, and

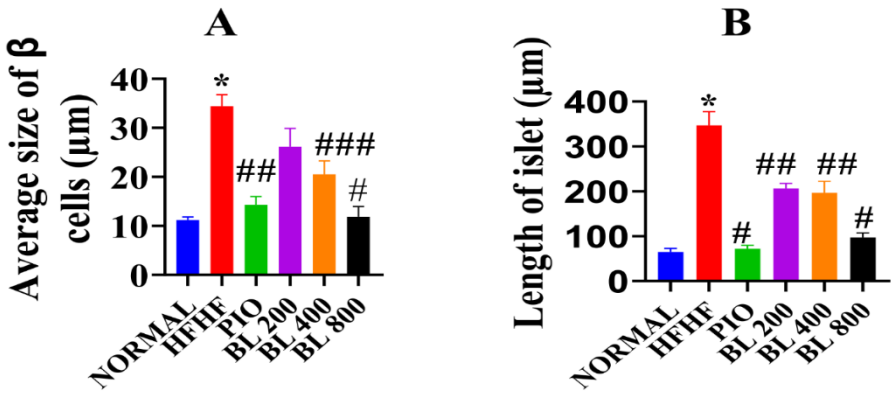


**Figure 7:** Histological changes in pancreas. A) Average size of β-cells; B) Length of islets. *$p$<0.001 vs. Normal group; #$p$<0.001, ##$p$<0.01, ###$p$<0.05 vs. HFHF group.

SOD) and reduced oxidative stress-related damage in the liver, as evidenced by histopathological analysis.[52]

The improvement in insulin resistance observed with BL treatment may be linked to its strong antioxidant potential, evidenced by increased levels of endogenous antioxidants, including Superoxide Dismutase (SOD) and reduced Glutathione (GSH).[53] Excessive generation of Reactive Oxygen Species (ROS) activates stress-sensitive kinases such as c-Jun N-terminal kinase (JNK) and inhibitor of nuclear factor Kappa-B Kinase β (IKK-β), which induce serine phosphorylation of Insulin Receptor Substrate-1 (IRS-1). This modification reduces insulin sensitivity in peripheral tissues, including skeletal muscle, liver, and adipose tissue, by impairing insulin signaling.[54]

By increasing the activities of SOD and GSH, BL likely attenuate ROS accumulation and lipid peroxidation, thus restoring the redox balance. The dismutation of superoxide anions into hydrogen peroxide is catalysed by SOD[55] which is subsequently detoxified by GSH-dependent peroxidases, ultimately protecting cells from oxidative damage. This antioxidant defence not only preserves pancreatic β-cell function by preventing oxidative apoptosis but also improves glucose uptake in peripheral tissues by allowing proper insulin receptor signaling.[56]

Moreover, phytoconstituents reported in BL such as phenolic acids, flavonoids, and tannins are known to exert free radical scavenging, metal-chelating, and anti-inflammatory properties, all of which contribute to reduced oxidative stress and improved insulin sensitivity.[57] Flavonoids such as quercetin analogues have been shown to upregulate PI3K/Akt signaling, enhance Glucose Transporter Type-4 (GLUT4) translocation[58] and suppress NF-κB–mediated inflammatory responses, collectively ameliorating insulin resistance.[59]

Thus, the antioxidant effect of BL, indicated by elevated SOD and GSH levels,[60] appears to be a critical mechanism by which the extract exerts its insulin-sensitizing action. These findings support the therapeutic potential of BL as a natural source of bioactive compounds for the management of insulin resistance and related metabolic disorders.[61]

The study's results demonstrate that BL's anti-IR activity involves a multi-target approach, including key proteins like PPARG, DPP4, and PTP1B. These targets correlate with improvements in insulin sensitivity, glucose uptake, and pancreatic and hepatic function.[62] The presence of bioactive flavonoids such as kaempferol-7-o'-glucoside, quercetin, and myricetin derivatives likely drives these effects. Prior studies support BL's potential as a natural therapeutic agent for IR and metabolic disorders.[63] On the other hand, further phytochemical profiling (HPLC, LC-MS/MS) are required to strengthen the translational relevance to confirm and quantify the identified bioactives. However, further molecular studies are necessary to validate these findings and explore their clinical implications comprehensively.

## CONCLUSION

The present study highlights flavonoids through a systems biology approach, from BL leaves as key bioactive compounds that interact with major molecular targets implicated in diabetes mellitus, including PPARG, DPP4, and PTPN1 and PI3K-Akt signaling pathway was identified as a critical mediator in regulating insulin resistance. *In vivo* results demonstrated that BL treatment effectively attenuated HFHF diet-induced metabolic alterations by reducing weight gain, improving glucose tolerance, and enhancing insulin sensitivity. These effects were accompanied by significant anti-inflammatory, antioxidant, antihyperglycaemic, and antihyperlipidaemic activities. Overall, the findings suggest that flavonoids present in BL leaves may exert their anti-insulin resistance effects by modulating PPARG, DPP4, and PTPN1, thereby enhancing insulin signaling via the PI3K-Akt pathway. To strengthen these mechanistic insights, further validation using isolated phytoconstituents or enriched fractions, Western blot or

qPCR need to be performed to validate the expression changes of key proteins in the PI3K-Akt pathway.

## ACKNOWLEDGEMENT

The authors express their sincere gratitude to Dr. Sunil S. Jalalpure, Principal of KLE College of Pharmacy, Belagavi, for his invaluable guidance and for providing the necessary resources. They also extend their heartfelt thanks to the Department of Pharmaceutics, Vasantidevi Patil Institute of Pharmacy, Kodoli, for their unwavering support in the successful completion of this research work.

## ABBREVIATIONS

**BL:** Methanolic extract of *Buchanania lanzan* leaves; **AMPK:** AMP-activated Protein Kinase; **CAT:** Catalase; **DAG:** Diacylglycerol; **DPP4**: Dipeptidyl Peptidase 4; **DM:** Diabetes mellitus; **FBG:** Fasting blood glucose; **FDR:** False discovery rate; **GLP:** Glucagon like peptide; **GLUT:** Glucose Transporter; **GSH:** Reduced glutathione; **HDL:** High Density Lipoprotein; **HFHF:** High Fat High Fructose; **IKK-β:** Inhibitor of nuclear factor kappa-B kinase β; **IRS-1:** Insulin receptor substrate-1; **IR:** Insulin resistance; **JNK:** c-Jun N-terminal kinase; **KEGG:** Kyoto Encyclopaedia of Genes and Genomes; **LDL:** Low Density Lipoprotein; **NAFLD:** Non-Alcoholic Fatty-Liver Disease; **OGTT:** Oral Glucose Tolerance Test; **PDB:** Protein data bank; **PI3K:**Phosphoinositide 3-Kinase; **PIO:** Pioglitazone; **PMBJP:** Pradhan Mantri Bhartiya Janaushadhi Pariyojana; **PPARG:** Peroxisome Proliferator-Activated Receptor Gamma; **PPI:** Protein-protein interactions; **PTPN1:** Protein Tyrosine Phosphatase Non-receptor Type 1; **qPCR:** Quantitative Polymerase Chain Reaction; **RCSB:** Research Collaboratory for Structural Bioinformatics; **SFA:** Saturated Fatty-Acids; **SOD:** Superoxide dismutase; **STRING:** Search tool for Retrieval of molecular-input line-entry system; **STZ:** Streptozotocin **T2DM:** Type 2 Diabetes Mellitus; **TFA:** Trans Fatty Acids; **TNF-α:** Tumor Necrosis Factor alpha; **VLDL:** Very Low Density Lipoprotein.

## CONFLICT OF INTEREST

The authors declare that there is no conflict of interest.

## ETHICS APPROVAL AND CONSENT TO PARTICIPATE

The Institutional Animal Ethics Committee (IAEC) at KLE College of Pharmacy Belagavi, approved the experimental procedures (Reg. No.: 221/Re/S/CPCSEA/2000), which complied with the ethical standards stipulated by the Committee for the Control and Supervision of Experiments on Animals (CPCSEA). Wistar rats weighing 180-200g were procured with approval from IAEC New Delhi.

## AUTHORS CONTRIBUTIONS

**Rubina U. Watangi**: Investigation, Methodology, Writing – original draft, review & editing Visualization, Validation, Conceptualization, Resources, Supervision, Project administration. **Nayeem A. Khatib:** Methodology, Writing – review & editing, Supervision, Visualization. **Tufail B. Sajjan, Ekta U. Kotharkar and Rajkumar S. Patil:** Monitoring animal studies and involved in performing and analysis the in-silico studies. **Arehalli S. Manjappa and Sunil T. Galatage:** Writing – review, editing.

## COLLECTION AND AUTHENTICATION OF PLANT MATERIAL

*Buchanania lanzan* leaves, were collected from Ajara Forest Region (Kolhapur district, Maharashtra, India) in May 2020 and recognized and verified by Dr. Harsha Hegde, ICMR, Belagavi and the herbarium voucher sample number RMRC-1602 was kept in pharmacognosy department of KLE College of Pharmacy, Belagavi.

## SUMMARY

The objective of this study is to evaluate methanolic extract of *Buchanania lanzan* leaves (BL) for insulin sensitivity in diet induced insulin resistance rats and to elucidate the mechanisms of *B. lanzan* leaves constituents with the support of computational tools. The PI3K-Akt signalling pathway was identified to score the highest gene count and lowest false discovery rate. Our findings confirmed that a BL showed anti-insulin resistance, anti-inflammatory, anti-hyperlipidaemia, anti-hyperglycaemic and, antioxidant activity might be due to presence of flavonoids. BL lowered elevated blood glucose levels by stimulating insulin secretion, played role in preserving liver and islet cell histology, regulating glycolysis or gluconeogenesis, increasing glucose uptake in skeletal muscles, and decreasing TNF-α levels in liver. Flavonoids in *Buchanania lanzan* leaves probably alter PPARG, DPP4, and PTPN1 proteins, enhancing insulin sensitivity via the PI3K-Akt signalling pathway.

## REFERENCES

1. Boucher J, Kleinridders A, Kahn CR. Insulin receptor signaling in normal. Cold Spring Harb Perspect Biol. 2014;6:a009191.
2. Chen CC, Lii CK, Lin YH, Shie PH, Yang YC. *Andrographis paniculata* improves insulin resistance in high-fat diet-induced obese mice and TNF-α-treated 3T3-L1 adipocytes. J Food Drug Anal. 2020;48(5):1073-90.
3. Kahn BB, Flier JS. Obesity and insulin resistance. J Clin Invest. 2000;106(4):473-81.
4. Manisha E, Amarjot G, Thakur K, Singh G, Bedi O. Pathobiological and molecular connections involved in high-fructose and high-fat diet-induced diabetes-associated NAFLD. Inflamm Res. 2020. Available from: https://doi.org/10.1007/s00011-020-01373-7
5. Ghee DV. Vanaspati: Desi vegetable ghee. 1990; 7-12.
6. Thompson AK, Minihane AM, Williams CM. Trans fatty acids, insulin resistance and diabetes. Eur J Clin Nutr. 2011;65:553-64.
7. Tupas GD, Otero MCB, Ebhohimen IE, Egbuna C, Aslam M. Antidiabetic lead compounds and targets for drug development. In: Phytochemicals as Lead Compounds for New Drug Discovery. Elsevier; 2020. p. 127-41.

8. Munshi RP, Joshi SG, Rane BN. Development of an experimental diet model in rats to study hyperlipidemia and insulin resistance. Indian J Pharmacol. 2014;46(3).
9. Hu F, Niu Y, Xu X, Hu Q, Su Q, Zhang H. Resistant dextrin improves high-fat-high-fructose diet-induced insulin resistance. Food Funct. 2020; 1-11.
10. Salehi B, Ata A, Kumar NVA, Sharopov F, Ramírez-Alarcón K, Ruiz-Ortega A, *et al.* Antidiabetic potential of medicinal plants and their active components. Biomolecules. 2019; 9.
11. Chhipa S, Sisodia SS. Indian medicinal plants with antidiabetic potential. J Drug Deliv Ther. 2019;9(1):257-65.
12. Bird SR, Hawley JA. Update on the effects of physical activity on insulin sensitivity in humans. Sports Med. 2016;46(9):1-26.
13. Sharma DR, Sharma A. *Buchanania lanzan* is a pharmacognostic miracle herb. Int J Pharm Sci. 2015; 1-6.
14. Sharan CD, Barkha C. Pharmacological importance of *Buchanania lanzan* Spreng. Int J Pharm Sci Res. 2019;1(2):25-8.
15. Sushma N, Smitha PV, Gopal YV, Vinay R, Srinivasa N. Antidiabetic, antihyperlipidemic and antioxidant activities of *Buchanania lanzan* methanol leaf extract in STZ-induced diabetic rats. Int J Pharm Pharm Sci. 2013;12:221-6.
16. Rajput BS, Gupta D, Kumar S, Singh K. *Buchanania lanzan*: a vulnerable multipurpose species. Int J Curr Microbiol App Sci. 2018;7(5):833-6.
17. Ahmad K, Shaikh S, Lim JH, Ahmad SS, Chun HJ, Lee EJ, *et al.* Therapeutic application of natural compounds for skeletal muscle-associated metabolic disorders: a review. Biomed Pharmacother. 2023;168:115642.
18. Samdani A, Vetrivel U. POAP: A GNU parallel-based multithreaded pipeline of Open Babel and AutoDock suite for boosted virtual screening. Comput Biol Chem. 2018;74:39-48.
19. Sushma N, Smitha PV, Gopal YV, Vinay R, Reddy NS, Mohan M, *et al.* Antidiabetic and antioxidant activities of *Buchanania lanzan*. Trop J Pharm Res. 2013;12(2):221-6.
20. Sornalakshmi V, Tresina SP, Paulpriya K, Lincy MP, Mohan VR. OGTT in glucose-induced hyperglycemic rats with *Hedyotis leschenaultiana*. Int J Toxicol Pharmacol Res. 2016;8(1):59-62.
21. Kumar R, Patel DK, Prasad SK, Sairam K, Hemalatha S. Antidiabetic activity of *Caesalpinia digyna* root extract. Asian Pac J Trop Biomed. 2012;2:S934-40.
22. Yoon H, Jeon DJ, Park CE, You HS, Moon AE. Association of HOMA-IR and β-cell function with vitamin D in Korean adults. J Clin Biochem Nutr. 2016;59(2):139-44.
23. Sinha AK. Colorimetric assay of catalase. Anal Biochem. 1972;47(2):389-94.
24. Pattanaik J, Chalakh S, Gandhi M. Evaluation of antivenom potential of Natakushtadi Yoga against cobra venom. Ann RSCB. 2021; 25.
25. Misra P. Superoxide dismutase. Anal Biochem. 1977; 1-5.
26. Sabu MC, Subburaju T. Effect of *Cassia auriculata* on glucose utilization. J Ethnopharmacol. 2002;80(2-3):203-6.
27. Siddiqui MZ, Roy A, Niranjan C. Phytochemical and antioxidant evaluation of *Buchanania lanzan* gum. Proc Nat Acad Sci India B. 2015.
28. Siddiqui MZ, Chowdhury AR, NP, MT. *Buchanania lanzan*: a species of enormous potential. World J Pharm Sci. 2014;2(4):374-9.
29. Chen C, Zhang Y, Huang C. Berberine inhibits PTP1B and mimics insulin. Biochem Biophys Res Commun. 2010;397(3):543-7.
30. Duraipandiyan V, Balamurugan R, Al-dhabi NA, Raja TW, Ganesan P, Ahilan B, *et al.* Downregulation of PTP1B and metabolic correction by *Borassus flabellifer* fruit extract. Saudi J Biol Sci. 2020;27(1):433-40.
31. Forouhi NG, Misra A, Mohan V, Taylor R. Dietary approaches for prevention of type 2 diabetes. Lancet Diabetes Endocrinol. 2018;6:93-4.
32. Sell H. Reduced DPP4 activity improves insulin signaling in human adipocytes. Biochem Biophys Res Commun. 2016;471:348-54.
33. Baumeier C, Schlüter L, Saussenthaler S, Laeger T, Rödiger M, Alaze SA, *et al.* Elevated hepatic DPP4 activity promotes insulin resistance and NAFLD. Mol Metab. 2017;6(10):1254-63.
34. Van Bloemendaal L, Kulve JS, de Fleur SE, Ijzerman RG, Diamant M. GLP-1 effects on appetite and body weight. Obes Rev. 2007;4:1-12.
35. Boucher J, Kleinridders A, Kahn CR. Insulin receptor signaling in normal and insulin-resistant states. Cold Spring Harb Perspect Biol. 2014;6:a009191.
36. Sajid M, Akash H. TNF-α: role in insulin resistance and type 2 diabetes. Crit Rev Eukaryot Gene Expr. 2017;27(3):247-53.
37. Jaiswal Y, Tatke P, Gabhe SY. Phytopharmacological profile of *Buchanania lanzan*. Asian Pac J Trop Biomed. 2014; 4(S1):S41-5.
38. Goyal PK, Chauhan A, Singh S. Phytochemistry and pharmacological activities of *Buchanania lanzan*. Int J Pharm Sci Res. 2019;10(5):2126-35.
39. Pal D, Mishra P, Sachan N. Pharmacological and phytochemical screening of *Buchanania lanzan*. J Pharm Res. 2011;4(2):421-4.
40. Evans JL, Goldfine ID, Maddux BA, Grodsky GM. Oxidative stress: a unifying hypothesis of type 2 diabetes. Endocr Rev. 2002;23(5):599-622.
41. Houstis N, Rosen ED, Lander ES. ROS have a causal role in insulin resistance. Nature. 2006;440(7086):944-8.
42. Henriksen EJ, Diamond-Stanic MK, Marchionne EM. Oxidative stress in insulin resistance. Free Radic Biol Med. 2011;51(5):993-9.
43. Joseph B, Jini D. Antidiabetic effects of flavonoids. Recent Pat Endocr Metab Immune Drug Discov. 2013;7(1):17-32.
44. Bahadoran Z, Mirmiran P, Azizi F. Dietary polyphenols in diabetes management. J Diabetes Metab Disord. 2013;12:43.
45. Yki-Järvinen H. Thiazolidinediones. N Engl J Med. 2004;351(11):1106-18.
46. Nissen SE, Wolski K. Rosiglitazone and cardiovascular risk. N Engl J Med. 2007;356(24):2457-71.
47. Dormandy JA, Charbonnel B, Eckland DJ, Erdmann E, *et al.* PROactive: pioglitazone clinical trial. Lancet. 2005;366:1279-89.
48. Soccio RE, Chen ER, Lazar MA. Thiazolidinediones and insulin sensitization. Cell Metab. 2014;20(4):573-91.
49. Yao M, Teng H, Lv Q, Gao H, Guo T, Lin Y, *et al.* Anti-hyperglycemic effects of dihydromyricetin. Food Sci Hum Wellness. 2021;10(2):155-62.
50. Plomgaard P, Bouzakri K, Krogh-Madsen R, Mittendorfer B, Zierath JR, Pedersen BK. TNF-α induces insulin resistance in humans via AS160 inhibition. Diabetes. 2005;54(10):2939-45.
51. Hurrle S, Hsu WH. Etiology of oxidative stress in insulin resistance. Biomed J. 2017;40(5):257-62.
52. Evans JL, Goldfine ID, Maddux BA, Grodsky GM. Oxidative stress and stress-activated pathways. Endocr Rev. 2002;23(5):599-622.
53. Houstis N, Rosen ED, Lander ES. ROS and insulin resistance. Nature. 2006;440:944-8.
54. Henriksen EJ, Diamond-Stanic MK, Marchionne EM. Oxidative stress and type 2 diabetes. Free Radic Biol Med. 2011;51:993-9.
55. Joseph B, Jini D. Antidiabetic flavonoids. Recent Pat Endocr Metab Immune Drug Discov. 2013;7:17-32.
56. Jaiswal Y, Tatke P, Gabhe SY. Phytopharmacological profile of *Buchanania lanzan*. Asian Pac J Trop Biomed. 2014; 4(S1):S41-5.
57. Goyal PK, Chauhan A, Singh S. Phytochemistry of *Buchanania lanzan*. Int J Pharm Sci Res. 2019;10:2126-35.
58. Bahadoran Z, Mirmiran P, Azizi F. Dietary polyphenols. J Diabetes Metab Disord. 2013;12:43.
59. Liu W, Zhai Y, Heng X, Che FY, Chen W, Sun D, *et al.* Oral bioavailability of curcumin. J Drug Target. 2014;24(8):694-702.
60. Chen L, Lin X, Fan X, Qian Y, Lv Q, Teng H. *Sonchus oleraceus* extract enhances glucose homeostasis via AMPK/Akt/GSK-3β pathway. Food Chem Toxicol. 2020;136:111072.
61. Alkhalidy H, Moore W, Zhang Y, McMillan R, Wang A, Ali M, *et al.* Kaempferol promotes insulin sensitivity and preserves β-cell mass in obese mice. Molecules. 2015; 2015:1-12.
62. Lee SB, Shin JS, Han HS, Lee HH, Park JC, Lee KT. Kaempferol 7-O-β-D-glucoside inhibits pro-inflammatory mediators. Chem Biol Interact. 2018;284:101-11.
63. Choi YH, Oh IY, Nguyen NM, Ko A, Choi JW, Park WJ, *et al.* Gallic acid regulates body weight and glucose homeostasis via AMPK activation. Endocrinology. 2015;156:157-68.


**Cite this article:** Watangi RU, Khatib NA, Galatage ST, Manjappa AS, Sajjan TB, Kotharkar EU, *et al*. Insulin-Sensitizing Effect of *Buchanania lanzan* Leaf Extract: Integrated Computational and *in vivo* Evidence. Indian J of Pharmaceutical Education and Research. 2026;60(3s):s1215-s1230.